ISSN: 2472-3703 DOI: 10.6911/WSRJ.202105_7(5).0027

Quinolone Based Squaraine Probe for A Dual Fluorescent Recognition of Fe^{3+} and Cu^{2+}

Xi Lu[1], Xiaoqian Liu[1, a]

[1]School of Pharmacy, Changzhou University, 213164, Jiangsu, China

[a]Email: chmliux@cczu.edu.cn

Abstract

A quinolone moiety as ion binding accepter was introduced into an asymmetric squaraine fluorophore by amide coupling reaction to obtain a new quinolone-squaraine based fluorescent chemosensor (ASQ). The sensor displayed an instant fluorescent response specific to Fe^{3+} (fluorescent enhancement) and Cu^{2+} (fluorescent quenching) over the other metal ions in Triton-100 (4 mM) surfactant solution. The limit of detection for Fe^{3+} was measured to be 81 nM and to be 10.6 nM for Cu^{2+}, respectively. Both detection limits were far lower than those in the environmental protection agency guideline (5.37 μM for Fe^{3+} and 20.5 μM for Cu^{2+}). The 1:1 stoichiometric ratio was determined by Job's plot analysis and the binding constant calculated by the Benesi-Hilderbrand plot revealed that the sensor ASQ had stronger binding affinity to Fe^{3+} instead of Cu^{2+}. The complexation mechanism was further proposed according to ESI-Mass and IR analysis. The coordination mode of ASQ-Fe^{3+} and ASQ-Cu^{2+} undergone two different pathways supported by DFT calculation. Finally, the ASQ sensor was successfully applied in the waste water sample analysis.

Keywords

Quinolone-squaraine structure; Dual fluorescent responses; Iron and copper detection; Low detection limit; Real sample application.

1. INTRODUCTION

Recently, the development of fluorescent chemosensor for metal ions detection has attracted great interests by researchers in the biology, chemistry, and environmental science [1-6]. Among various metal ions, iron is considered as a ubiquitous metal as it plays an important role in cellular metabolism, oxygen carrying and regulation of enzyme reactions [7-13]. Either deficiency or excess in the body can induce dysfunction of organs including heart, pancreas and liver. Similarly, copper as the third most abundant essential trace element plays a critical role in metabolic process as well [14-17]. Either its deficiency or overdose can induce the imbalance of homeostasis, resulting in severe diseases including Alzheimer's, Parkinson's diseases [18-20]. Current techniques for Fe^{3+} and Cu^{2+} detections are involved in atomic absorption spectroscopy, inductively coupled plasma mass spectroscopy, electrochemical analysis [21-25]. However, these require sophisticated instruments, tedious sample preparation and trained personnel which limit their wide applications. Thus, fluorescent chemosensor with obvious advantages in high sensitivity and selectivity, cost-effective, rapid response and low detection limit is highly in demand. So far, various fluorescent sensors based on organic chromophores have been designed for Fe^{3+} and Cu^{2+} [26-38]. Many reported examples exhibited fluorescent "on-off" behavior due to their paramagnetic natures and only can provide one-to-one analysis. Some of the examples had limitations in the sense of cross sensitivity, slow response and high detection limit, which restricted their practical applications. Recently, dual ion chemosensors have

ISSN: 2472-3703 DOI: 10.6911/WSRJ.202105_7(5).0027

emerged and gradually become a new research interest. They are based on a single host that can independently recognize two ion species and provide distinct spectral responses via the same or different channels in one system. This allows minimizing the high cost of synthesis and accelerating the analysis process. A few examples have been reported to achieve multiple ions detections [39]. However, examples for dual-analyte detection of Fe^{3+} and Cu^{2+} in one system are relatively rare and only a few examples containing pure organic chromophores were reported recently. However, some suffered from both fluorescent quenching phenomenon and some required organic solvent for the dual detection of Fe^{3+} and Cu^{2+} [40]. The detection limits in these cases were relatively high as well, which restricted their further applications. In this context, the design and synthesis of facile, low cost fluorescent sensors for dual recognition of Fe^{3+} and Cu^{2+} with high selectivity and sensitivity remains a challenge.

Squaraines are fluorescent dyes with sharp and intense absorption and fluorescent emission in the near infrared region [41]. The electron charge transfer can be occurred extensively in the donor-acceptor-donor conjugated structure. The coordination with certain metal ions results in the absorption and fluorescence change of squaraines [42]. Besides, the optical properties of squaraines can be affected by change in polarity and pH of solvent, temperature or the addition of additives as well.

All these features make squaraines especially suitable in the design of chemosensor.

We are gratifying to present a quinolone-squaraine based chemosensor which can independently recognize two ion species in one solution at the same time. It has not only shown "turn-on" fluorescent recognition for Fe^{3+} but also expressed a "turn-off" fluorescent selectivity for Cu^{2+} in Triton-100 aqueous solution. The limit of detection for Fe^{3+} was measured to be 81 nM and to be 10.6 nM for Cu^{2+}, respectively. Both detection limits were far lower than those in the environmental protection agency guideline (5.37 uM for Fe^{3+} and 20.5 μM for Cu^{2+}) and superior to most reported examples. The proposed complexation mechanism for both Fe^{3+} and Cu^{2+} was suggested undergo a different way. The excellent selectivity for Fe^{3+} in fluorescence enhancement was owing to the formation of rigid structure for ASQ-Fe^{3+} complex, while the fluorescence quenching for Cu^{2+} could be ascribed to the photo induced electron transfer (PET) effect in the chelation of ASQ-Cu^{2+} complex. These findings were further supported by IR analysis and DFT calculation. Lastly, the ASQ sensor has proven to be successful in the analysis of waste water samples.

2. EXPERIMENTAL SECTION

2.1. Materials and Instrumentation

Unless stated, all the chemicals and solvent used were purchased from commercial sources without purification. 1H NMR (400 MHz) and ^{13}C NMR (400 MHz) spectra were recorded on a Bruker AV-400 spectrometer (TMS as internal standard). Electrospray ionization mass spectra (ESI-MS) were performed using a DECAX-3000 LCQ Deca XP ion trap mass spectrometer. FT-IR spectra were recorded using a PerkinElmer Spectrum 2000 Fourier Transform Infrared Spectrophotometer. Absorption and fluorescent spectra were measured on Molecular Device Spectrometer 5 (Molecular Devices Corporation, USA).

2.2. General Procedures for UV-vis Experiments

A stock solution of ASQ was prepared 10 mM in DMSO. Further dilutions were made to prepare 100 μM of ASQ by diluting with different solutions. Heavy metal ions stock solution including Na^{+}, K^{+}, Li^{+}, Fe^{3+}, Ag^{+}, Zn^{2+}, Hg^{2+}, Cd^{2+}, Fe^{2+}, Co^{2+}, Ca^{2+}, Cu^{2+} were prepared 10 mM in distilled water and diluted further accordingly. 2 μL of ASQ in stock solution (10 mM) and 2 μL of metal ion stock solution (10 mM) were extracted and mixed together, followed by diluting with 196 μL solvents to make total volume of 200 μL. In this condition, the final concentration

ISSN: 2472-3703 DOI: 10.6911/WSRJ.202105_7(5).0027

of ASQ and metal ions were 100 μM, individually. The solution was transferred into 96 well plates on Molecular Device Spectrometer 5 (Molecular Devices Corporation, USA) and the absorption measurements were made at the wavelength range of 350 nm to 750 nm.

2.3. General Procedures for Fluorescence Measurements

The sample preparation procedures were the same as those for UV-vis experiments. The fluorescence measurements were carried out on Molecular Device Spectrometer 5 (Molecular Devices Corporation, USA) with excitation wavelength of 635 nm and emission wavelength of 665 nm.

2.4. Compound Synthesis

2.4.1 Synthesis of 2-Chloro-N-(quinloline-8yl)acetamide (1)

A cool mixture solution of 8-aminoquinoline (0.144 g, 1 mmol) and trimethylamine (0.68 mL, 5 mmol) was added dropwise of 2-chloroacetyl chloride (370 μL, 5 mmol) in dichloromethane (10 mL). The reaction mixture was stirred for 4 hours and the crude yellow solid was purified by silica gel column chromatography using DCM:EA = 1:1 as eluent to obtain final product in yield of 85.0%. 1 was confirmed by NMR and ESI-MS. 1H NMR (400 MHz, $CDCl_3$) δ: 10.92 (s, 1H), 8.88-8.87 (dd, *J* = 1.6 Hz, 1H), 8.78-8.76 (m, 1H), 8.20-8.18 (dd, *J* = 2.0 Hz, 1H), 7.59-7.56 (m, 2H), 7.51-7.49 (m, 1H), 4.33-4.32 (d, *J* = 1.6 Hz, 2H). ^{13}C NMR (100 MHz, $CDCl_3$) δ: 164.32, 148.54, 138.64, 136.24, 133.49, 127.88, 127.10, 122.48, 12.74, 116.64, 43.32. ESI-MS calculated for: 220.04; found: 221.20.

2.4.2 Synthesis of 2-(4-Amino-phenylamino)-N-quinolin-8-yl Acetamide (2)

The compound 2 was synthesized by refluxing 1 (0.15 g, 0.68 mmol) and p-phenylenediamine (0.075 g, 0.68 mmol) with addition of K_2CO_3 (0.25 g, 0.68 mmol) and catalytic amount of KI in acetonitrile for overnight. The product was obtained by silica gel column chromatography purification using DCM:EA = 1:1 as eluent in the yield of 46.2% (0.092 g). The compound was confirmed by NMR and ESI-MS. 1H NMR (400 MHz, CDCl3) δ: 10.95 (s, 1H), 8.85-8.83 (dd, *J* = 1.6 Hz, 1H), 8.74-8.73 (dd, *J* = 1.6 Hz, 1H), 8.13-8.10 (dd, *J* =2.0 Hz, 1H), 7.54-7.41 (m, 2H), 7.40-7.39 (d, *J* = 4.0 Hz, 1H), 6.66-6.60 (m, 4H), 5.30 (s, 1H), 4.00 (s, 1H). ^{13}C NMR (100 MHz, $CDCl_3$) δ: 169.96, 140.27, 139.04, 138.73, 136.09, 134.05, 127.93, 127.16, 121.83, 121.49, 116.67, 115.18, 51.15. ESI-MS calculated for: 292.13; found: 293.20.

2.4.3 Synthesis of ASQ

ASQ was synthesized by the amide coupling reaction of compound 2 (0.292 g, 1 mmol) and asymmetrical squaraine (0.631 g, 1 mmol) mixtures in N,N-dimethylformamide (20 mL) together with amide coupling reagents of N, N-diisopropylethylamine (0.155 g, 1.2 mmol), benzotriazole 1-yl-oxytripyrrol idinophosphonium hexafluorophosphate (0.624 g, 1.2 mmol) for 4 hours at room temperature. It was monitored by thin layer chromatography and purified by column chromatography using DCM:MeOH = 30:1 as eluent. The final compound ASQ was obtained as dark solid in the yield of 52.0%. ASQ was confirmed by NMR and ESI-MS. 1H NMR (400 MHz, $CDCl_3$) δ: 8.84-8.81 (m, 1H), 8.73-8.72 (d, *J* = 3.3 Hz, 1H), 8.20-8.18 (d, *J* = 8.2 Hz, 1H), 8.13-8.11 (d, *J* = 7.8 Hz, 1H), 7.93-7.86 (m, 4H), 7.61-7.28 (m, 9H), 6.96-6.94 (d, *J* = 8.6 Hz, 1H), 6.80-6.78 (d, *J* = 8.8 Hz, 1H), 6.07 (s, 1H), 5.98 (s, 1H), 4.64 (s, 1H), 4.21 (s, 2H), 4.10-4.09 (d, *J* = 4.8 Hz, 2H), 3.92 (s, 2H), 2.63 (s, 2H), 2.06 (s, 6H), 1.82 (s, 6H), 1.44-1.43 (m, 3H), 1.32-1.27 (m, 12H), 0.89-0.86 (m, 3H). ^{13}C NMR (100 MHz, $CDCl_3$) δ: 172.92, 169.35, 168.21, 165.09, 148.48, 145.48, 144.39, 142.21, 138.72, 138.67,136.11, 135.10, 133.94, 131.56, 130.07, 129.87, 129.70, 128.58, 127.93, 127.44, 127.15, 124.68, 122.58, 122.52, 121.94, 121.55, 121.19, 116.66, 115.43, 113.80, 109.98, 108.55, 87.48, 86.61, 51.63, 50.11, 48.61, 43.63, 40.93, 38.91, 31.88, 31.67,

ISSN: 2472-3703 DOI: 10.6911/WSRJ.202105_7(5).0027

29.64, 29.27, 29.10, 27.25, 27.17, 27.01, 26.92, 26.51, 22.53, 14.04, 14.00, 12.39. ESI-MS calculated for: 904.4676; found: 905.4702.

2.5. Job's Plot Measurements

For Fe^{3+}, 0.2 μL, 0.4 μL, 0.6 μL, 0.8 μL, 1.0 μL, 1.2 μL, 1.4 μL, 1.6 μL, 1.8 μL of the sensor ASQ (10 mMsolution were taken and transferred to the vials. 1.8 μL, 1.6 μL, 1.4 μL, 1.2 μL, 1.0 μL, 0.8 μL, 0.6 μL, 0.4 μL, 0.2 μL of $FeCl_3$ (10 mM) were added subsequently to each sensor solution and Triton-100 (4 mM) were filled up accordingly to make a total volume of 200 uL in each, separately. After stirring for a few seconds, the fluorescence spectra were recorded with excitation wavelength of 635 nm. The plots were drawn by plotting 1/ ($I-I_o$) vs 1/[Fe^{3+}], where Io equaled to fluorescent intensity of ASQ without Fe^{3+}, I was corresponding to the fluorescent intensity of ASQ with different concentrations of Fe^{3+}. For Cu^{2+}, the procedures were similar as above.

2.6. Competition Tests

For Fe^{3+}, 2 μL Fe^{3+} (2 mM), 2 μL ASQ (10 mM) were extracted and mixed into vials. 2 μL of Na^+, K^+, Li^+, Ag^+, Zn^{2+}, Hg^{2+}, Cd^{2+}, Fe^{2+}, Co^{2+}, Ca^{2+} ion solutions (10 mM) was then added in and Triton-100 (4 mM) were filled up to total volume of 200 μL in each. After stirring for a few seconds, fluorescent spectra were recorded at room temperature. For the case of Cu^{2+}, the procedures were the same as above.

3. RESULTES AND DISCUSSION

3.1. Synthesis of ASQ

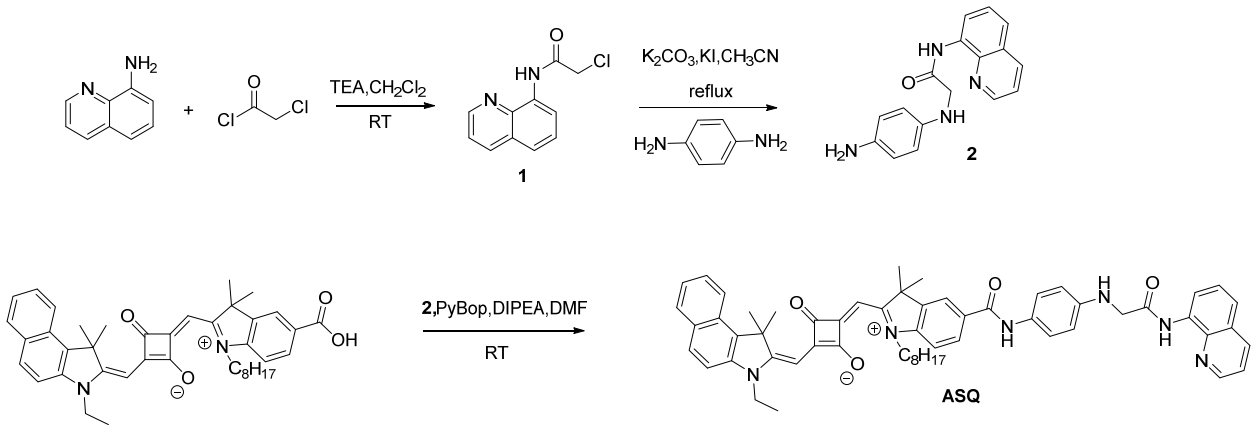

Scheme 1. Synthetic pathway for ASQ.

The synthesis of ASQ was illustrated in Scheme 1. 8-amino-quinoline was selected as the metal ion ligand and it was incorporated into asymmetrical squaraine though p-phenylenediamine as a linker. The final product was obtained as blue solid in good yield by amide coupling reaction and it has been confirmed and characterized by NMR and ESI-MS.

3.2. Sensing Properties of ASQ towards Fe^{3+} and Cu^{2+}

To evaluate the sensing properties of ASQ towards various metal ions, the absorption spectra of ASQ (10 mM) was firstly investigated. Four different aqueous solutions including distilled water and three surfactant solutions were applied as solvents. As shown in Figure 1, ASQ was very sensitive to the solvent environments. A broaden band with lower absorption intensity was observed when ASQ (final concentration: 100 μM) was in the distilled water or in the cationic surfactant hexadecyl trimethyl ammonium bromide (CTAB, 4 mM) solution. ASQ in the anionic

ISSN: 2472-3703 DOI: 10.6911/WSRJ.202105_7(5).0027

surfactant sodium dodecyl sulfonate (SDS, 4 mM) gave absorption responses with two maximum absorption peaks individually at 625 nm and 670 nm. Only a sharp and strong absorption band at 660 nm was observed for ASQ in the presence of 4 mM Triton-100 as non-ionic surfactant solution. As preliminary results have shown that ASQ could possess good absorption properties in 4 mM Triton-100, the Trixon-100 aqueous solution was selected as solvent for identifying the metal ions in the following experiments. 12 metal ion solutions including Na^{+}, K^{+}, Li^{+}, Ag^{+}, Zn^{2+}, Hg^{2+}, Cd^{2+}, Fe^{2+}, Co^{2+}, Ca^{2+}, Fe^{3+}, Cu^{2+} were added in to explore the recognition property of ASQ towards metal ions by measuring the absorption and emission spectra in Triton-100 (4 mM) solution. There were no significant absorption changes in the presence of all the metal ions compared to absorption spectrum of ASQ without metal ions (Figure 2a). However, ASQ exhibited distinct fluorescent changes toward Fe^{3+} and Cu^{2+} (Fig. 2b). The fluorescent intensity at maximum fluorescent peak of 670 nm was dramatically increased towards Fe^{3+}, while a significance decrement of fluorescent peak at same wavelength was observed for Cu^{2+}. To evaluate the surfactant effect on the Fe^{3+} detection, a range concentration (1 mM-10 mM) of Triton-100 solutions were adopted to tune the solvent environment of ASQ in the Fe^{3+} detection. As shown in Figure 3a, the fluorescence intensities for both ASQ and ASQ-Fe^{3+} were increased accompanied by the increasing concentrations of Triton-100. The fluorescent performance distinguished the most for Fe^{3+} detection in 4 mM Triton-100 with or without Fe^{3+}. In addition, the surfactant effect on the Cu^{2+} detection was investigated as well. A shown in Figure 3b, the fluorescent intensity of ASQ itself was dramatically increased when the concentration of Triton-100 was above 4 mM. Meanwhile, the fluorescent quenching was observed after addition of Cu^{2+} and no surfactant effect was found in the whole concentration ranges of Triton-100 for the ASQ-Cu^{2+} complex. Considering the consistency of solvent used in the dual ions detection, 4 mM Triton-100 was determined to use in the following study for the complex formation of ASQ towards Fe^{3+} and Cu^{2+}.

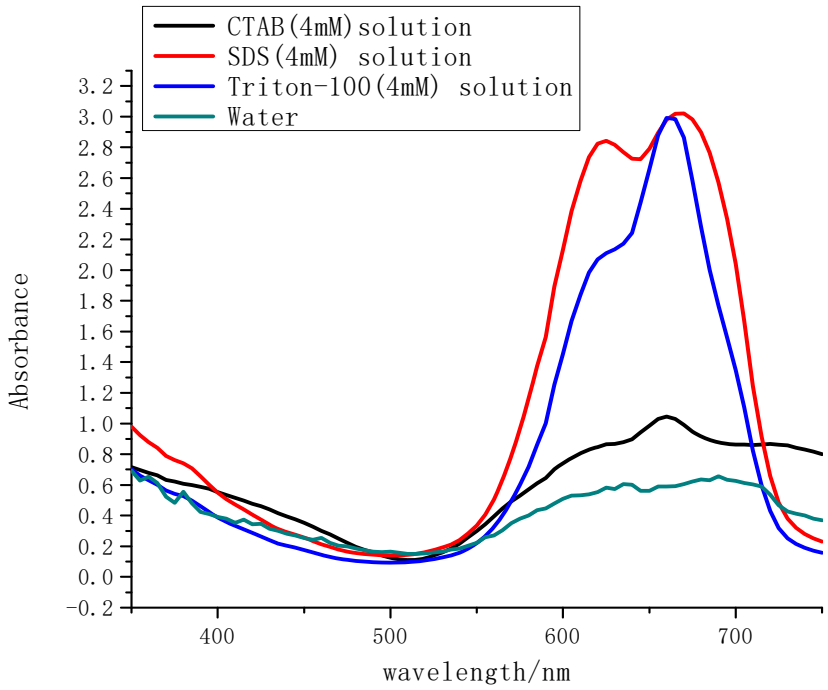

Figure 1. The absorption spectra of ASQ (100 μM) in different solutions

ISSN: 2472-3703 DOI: 10.6911/WSRJ.202105_7(5).0027

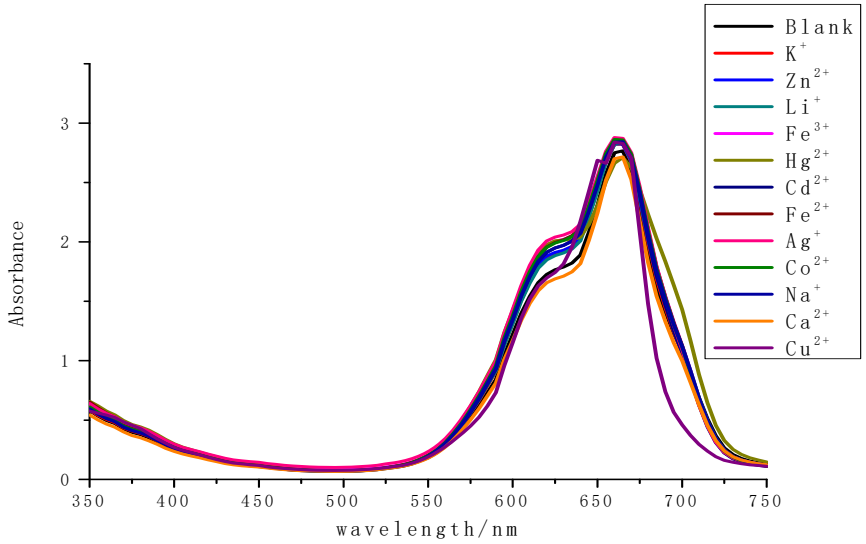

Figure 2a. Absorption spectra for ASQ solution (100 μM). with/without addition of different metal ions (100 μM) in Triton-100 (4 mM)

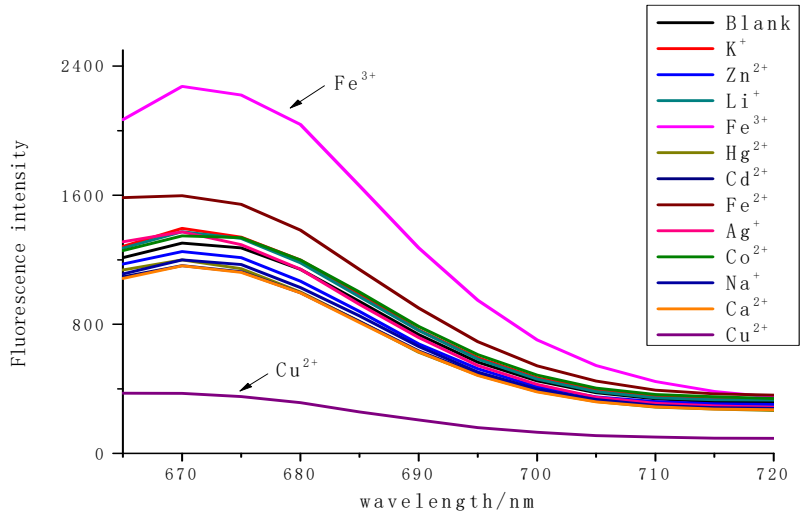

Figure 2b. Fluorescence spectra for ASQ solution (100 μM) with/without addition of different metal ions (100 μM) in Triton-100 (4 mM). lex = 635 nm, lem = 665 nm

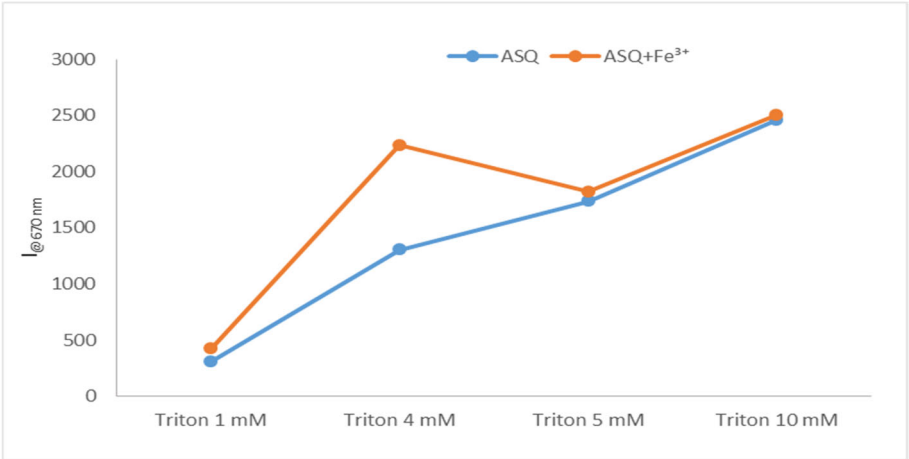

Figure 3a. Surfactant effects in Triton-100 for the ASQ (100 μM) fluorescence changes with or without addition of Fe^{3+} (100 μM)

ISSN: 2472-3703 DOI: 10.6911/WSRJ.202105_7(5).0027

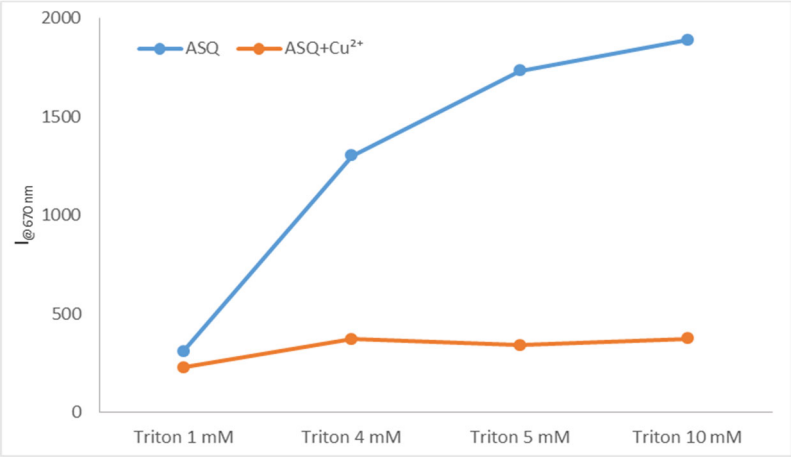

Figure 3b. Surfactant effects in Triton-100 for the ASQ (100 μM) fluorescence changes with or without addition of Cu^{2+} (100 μM)

To validate the selectivity for Fe^{3+} and Cu^{2+}, respectively, the competition experiments have also been performed. Other cations as interferences were added consequently into ASQ-Fe^{3+} and ASQ-Cu^{2+} complex solutions, respectively. The concentration of interferences was 5 times more than that of Fe^{3+} and Cu^{2+} in the complex.

As shown in Figure 4a, with addition of extra ions as interferences, the fluorescent quenching was observed in the solution (blue bar) which suggested the ASQ-Fe^{3+} complex was quite sensitive, while the fluorescence results in Figure 4b revealed that the presence of the other cations even at large extra amounts did not interfere with the determination of the presence and the amount of Cu^{2+} ion. All these findings suggest ASQ exhibit high selectivity for Fe^{3+} and Cu^{2+} compared to other metal ions and it could be used as a fluorescent chemosensor for dual analytes analysis.

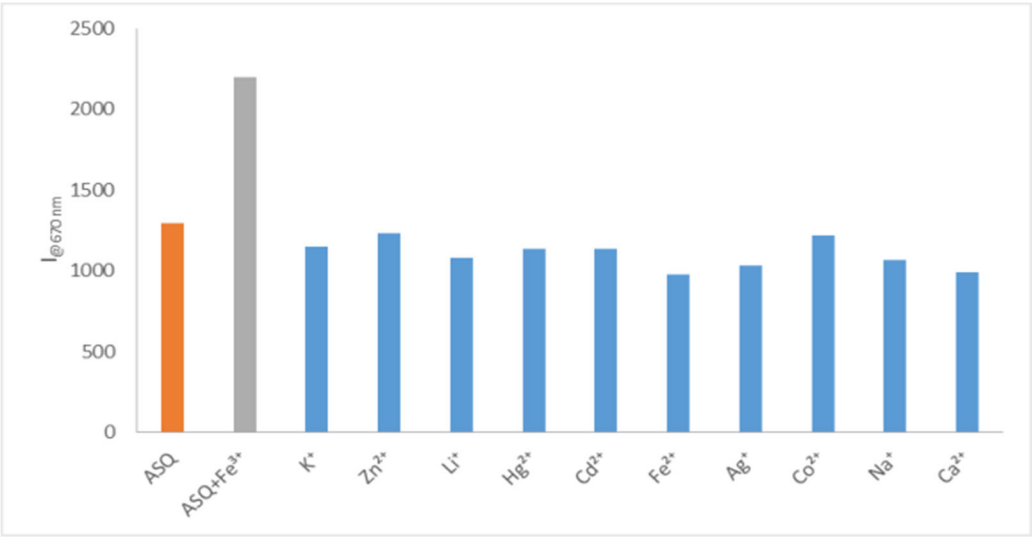

Figure 4a. Competition experiment of Fe^{3+} with other metal ions. Orange bar: fluorescence intensity of ASQ (4 mM). Gray bar: fluorescence intensity of ASQ (100 μM) with Fe^{3+} (100 μM) in Triton-100 (4 mM) solution. Blue bar: fluorescence intensity of ASQ (100 μM) with the addition of the Fe^{3+} (20 μM) in Triton-100 (4 mM) solution followed by the addition of respective competing cations (100 μM).

ISSN: 2472-3703 DOI: 10.6911/WSRJ.202105_7(5).0027

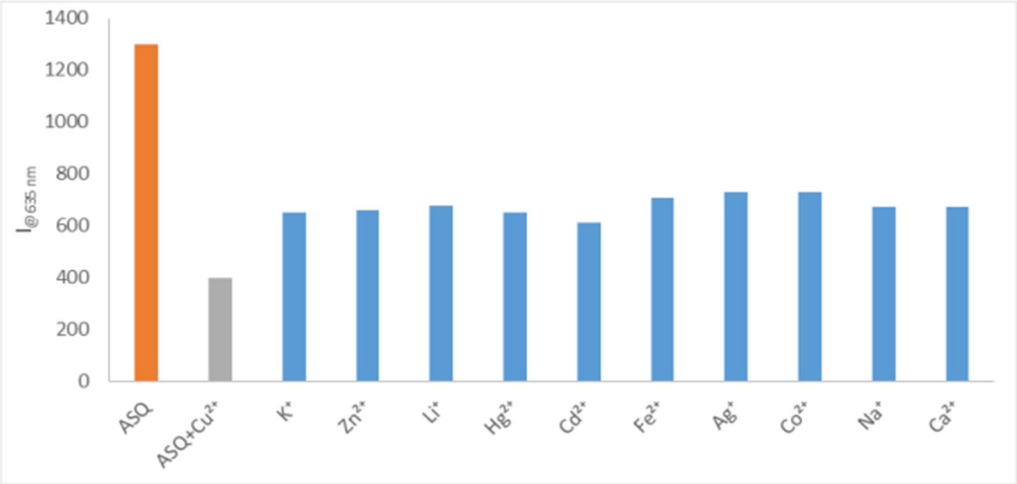

Figure 4b. Competition experiment of Cu^{2+} with other metal ions. Orange bar: fluorescence intensity of ASQ (4 mM). Gray bar: fluorescence intensity of ASQ (100 μM) with Cu^{2+} (100 μM) in Triton-100 (4 mM) solution. Blue bar: fluorescence intensity of ASQ (100 μM) with the addition of the Cu^{2+} (20 μM) in Triton-100 (4 mM) solution followed by the addition of respective competing cations (100 μM)

3.3. Binding Constant (Ka) and Limit of Detection (LOD) for Fe^{3+} and Cu^{2+}

To get a further insight into the fluorescence sensing properties of ASQ, a quantative titration for ASQ with Fe^{3+} and Cu^{2+} was carried out, respectively. With a continuous variation in the concentration of Fe^{3+}, the enhancement of fluorescence intensity at 670 nm was observed and it was steady after addition of 100 μM Fe^{3+} in 4 mM Triton-100. More importantly, the fluorescence enhancement of ASQ was corresponded to the concentration of Fe^{3+} in a linear manner in the range of 1 μM to 100 μM (R^2 = 0.9915, Figure 5a). The limit of detection (LOD) was calculated to be 81 nM in terms of the equation of detection limit = 3σ/k, where σ was standard deviation for ASQ, and k was the slop of standard curve between the fluorescence increment at 670 nm versus the concentration of Fe^{3+}. The limit of detection was at nmol level and far lower than the maximum allowed levels of Fe^{3+} in drinking water by the U.S. EPA (5.37 μM).

In addition, Job's plot measurement showed a maximum emission intensity value at a molar fraction of 0.5, which gave a solid evidence for the formation of 1:1 complex of ASQ-Fe^{3+} (Figure 5b). The complex was further confirmed by ESI-MS data. A solution containing ASQ and 1equivalent of Fe^{3+} has shown a strong peak at m/z: 994.9411, assigned to [ASQ+Fe^{3+}-3H^-] ion.

The binding constant (Ka) of ASQ-Fe^{3+} was estimated using a Benesi-Hilderbrand plot, which was calculated by fluorescence changes of consequent titration ($1/I-I_0$) against $1/[Fe^{3+}]$. The magnitude of Ka was calculated from the intercept and slope of the straight line, and the value was about 2.1×10^6 M^{-1}, which has shown a strong binding affinity to the ASQ-Fe^{3+} complex (Figure 5c).

The similar methods were applied to investigate the fluorescence sensing properties of ASQ to Cu^{2+} ion. With a continuous variation in the concentration of Cu^{2+}, the quenching of fluorescence intensity at 670 nm was observed and it was corresponded to the concentration of Cu^{2+} in a linear manner at the range of 0.1 μM to 10 μM (R^2 = 0.9925, Figure 5d). The detection limit was calculated to be 10.6 nM, which was far lower than that in the environmental protection agency guideline (20.5 μM for Cu^{2+}). In addition, maximum fluorescence intensity was found at a mole fraction of 0.5, which indicating the 1:1 stoichiometry between ASQ and Cu^{2+} (Figure 5e). The ESI-MS was found to be 1002.9885, which assigned to [ASQ+Cu^{2+}+Cl^-]$^+$ ion. The binding constant (Ka) of ASQ-Cu^{2+} was estimated to be 3.1×10^5 M^{-1} using a Benesi-

ISSN: 2472-3703 DOI: 10.6911/WSRJ.202105_7(5).0027

Hilderbrand plot analysis (Figure 5f), which has shown weaker binding affinity compared to that of ASQ-Fe^{3+}. The sensor ASQ has exhibited superior ability for Fe^{3+} and Cu^{2+} simultaneously in one solvent system.

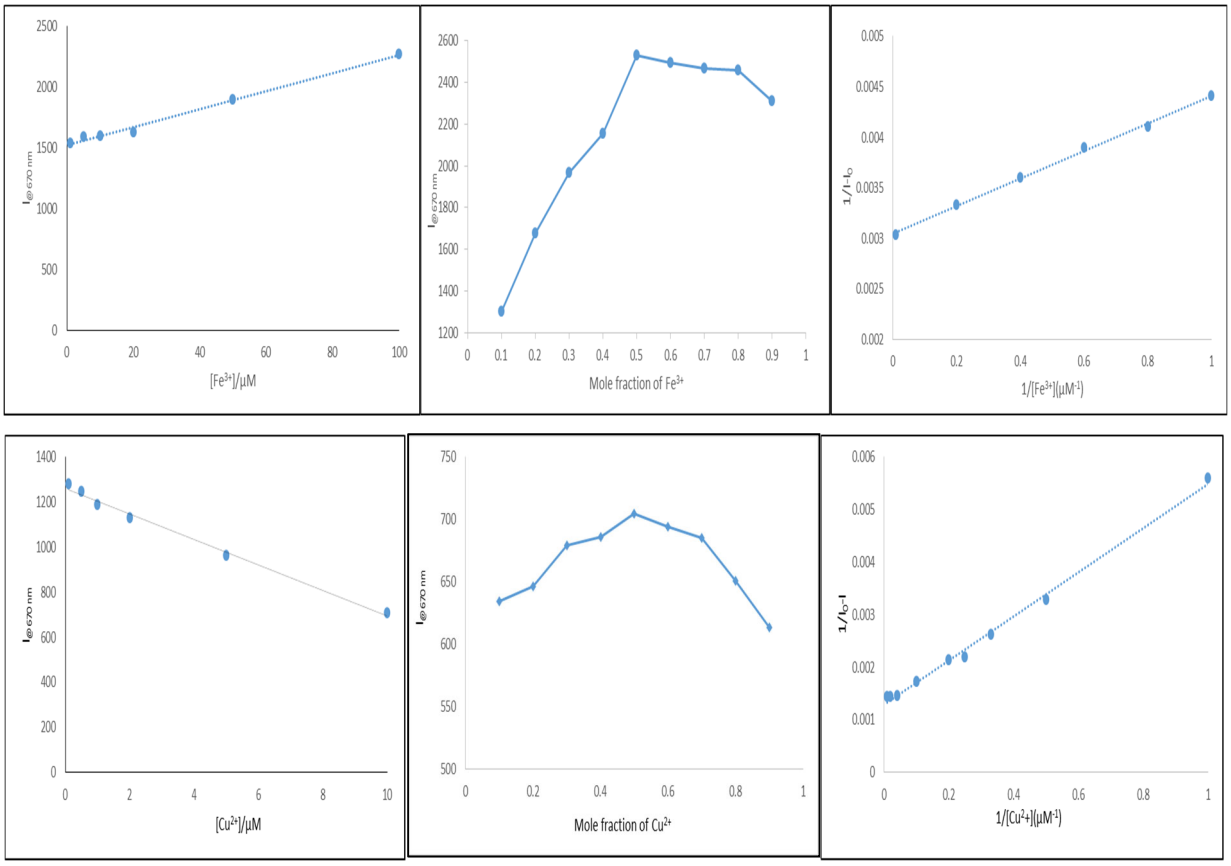

Figure 5 (a). The calibrated curve, which was plotted with the fluorescence intensity vs. Fe^{3+} concentrations (1-100 μM) at maximum emission wavelength, Y = 7.4109X + 1525.8, R^2 = 0.9915 **(b).** Job's plot for the complexation of ASQ with Fe^{3+} in Triton-100 (4 mM) solution **(c).** Benesi-Hildebrand plot analysis of the fluorescence changes for the complexation between ASQ and Fe^{3+}, R^2 = 0.9971 **(d).** The calibrated curve, which was plotted with the fluorescence intensity vs. Cu2+ concentrations (0.1-10 μM) at maximum emission wavelength, Y =-56.585X + 1261.8, R^2 = 0.9925 **(e).** Job's plot for the complexation of ASQ with Cu2+ in Triton-100 (4 mM) solution **(f).** Benesi-Hildebrand plot analysis of the fluorescence changes for the complexation between ASQ and Cu^{2+}, R^2 = 0.9955.

3.4. Complexation Mechanism of ASQ-Fe^{3+} and ASQ-Cu^{2+}

To gain additional insight into the binding of ASQ-Fe^{3+} and ASQ-Cu^{2+} complex, the FT-IR spectra of ASQ, ASQ-Fe^{3+} and ASQ-Cu^{2+} were carried out (Figure 6). The IR spectrum of ASQ exhibited amide N-H stretching band at 3326.83 cm^{-1}, methylene -CH_2 group aside the amide bond at 2926.18 cm^{-1} and 2851.46 cm^{-1}, carbonyl C=O stretching band at 1585.59 cm^{-1} and C-N bond in amide group assigned to 1493.50cm^{-1} and 1455.44 cm^{-1}, respectively. Upon complexation with Fe^{3+}, a broad stretching vibration band at 3357.27 cm^{-1} appealed and at the same time, the signal of the carbonyl C=O stretching band at 1584.22 cm^{-1} became stronger which indicating that the C=O group may participate in the complexation. When ASQ was coordinated with Cu^{2+}, the IR spectrum showed an even broad stretching vibration band around 3504.84 cm-1 and the signal of carbonyl C=O stretching band became weaker. Considered ASQ binding with Fe^{3+} and Cu^{2+} both in 1:1 stoichiometry, but has shown distinct IR spectrum, we

ISSN: 2472-3703 DOI: 10.6911/WSRJ.202105_7(5).0027

expect the ASQ-Fe^{3+} and ASQ-Cu^{2+} may undergo a different binding pathway. In ASQ-Fe^{3+} complex, nitrogen atoms on 8-aminoquinoline and on substituted p-phenylenediamine could be strong nucleophiles and act as electron donors to multiple coordinate with electron deficient iron ions together with carbonyl C=O aside involved. The fluorescence enhancement of the complex may be ascribed to the solid planarity and rigidity after complexation, which could also reduce the non-radiative decay of the excited state and lead to the pronounced fluorescence enhancement. For ASQ-Cu^{2+} complex, it was expected that N-H groups on substituted p-phenylenediamine aside the C=O carbonyl group involved in the complexation. It was believed that the mechanism of quenching effect of the ASQ-Cu^{2+} complex may be attributed to flexibility of the C=O carbonyl group in aminoquinoline and the electron transfer between Cu^{2+} ion and the excited ASQ.

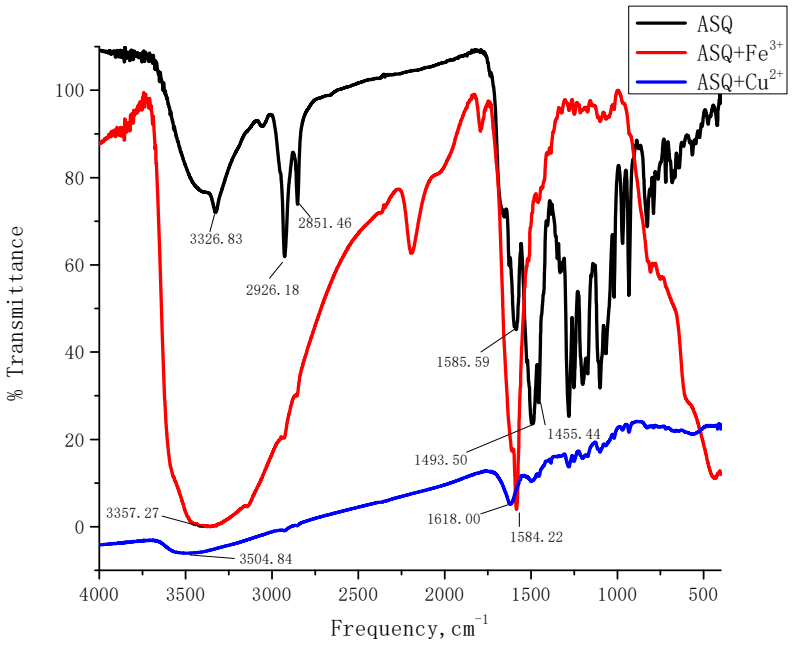

Figure 6. The IR spectrum of (a) ASQ, (b)A SQ-Fe^{3+} and (c) ASQ-Cu^{2+} complex in the soild state

3.5. Preliminary Analytical Applications

For practical applications, the sensor ASQ has been validated in the determination of Fe^{3+} and Cu^{2+} in the industrial waters. All the water samples were filtered through membrane and treated with 4 mM Triton-100 solution. They were then analyzed by sensor ASQ with results summarized in Table 1. Compared to the results measured by atomic absorption spectroscopy (AAS), the results by using our ASQ sensor were consistent with those by instrumental analysis, whereas the relative errors range from 1.40% to 2.83%. The analytical results obtained by sensor ASQ with excellent accuracy and reliability preliminarily demonstrated that it could be potential useful tool for determining Fe^{3+} and Cu^{2+} in real water samples.

Table 1. Determination of Fe^{3+} and Cu^{2+} in waste water samples

Industry waste water samples	Determined by AAS (μM)	ASQ (μM)	Relative erorr (%)
Sample 1	1.17±0.03	1.20±0.07 (Fe^{3+})	2.52
	1.21±0.02	1.18±0.05 (Cu^{2+})	-2.54
Sample 2	2.18±0.12	2.12±0.17 (Fe^{3+})	-2.83
	2.17±0.14	2.14±0.16 (Cu^{2+})	-1.4
Sample 3	4.20±0.18	4.32±0.24 (Fe^{3+})	2.78
	3.25±0.16	3.31±0.19 (Cu^{2+})	1.81

ISSN: 2472-3703 DOI: 10.6911/WSRJ.202105_7(5).0027

4. CONCLUSION

In summary, a new 8-aminoquinoline derived squaraine sensor ASQ has been developed to dual-responsive fluorescent recognition of Fe^{3+} and Cu^{2+} with high sensitivity and selectivity. The limit of detection for Fe^{3+} and Cu^{2+} were 81 nM and 10.6 nM, respectively. It exhibited better fluorescence performances in limit of detection and instant response compared to those literatures reported sensors. The binding mechanisms of ASQ-Fe^{3+} and ASQ-Cu^{2+} were confirmed undergoing two different pathways, which were supported by Job's plot analysis and FT-IR analysis calculation. Moreover, sensor ASQ was successfully used for on-site detection of Fe^{3+} and Cu^{2+} in real water samples with good excellent accuracy and reliability.

5. CONFLICTS OF INTEREST

There are no conflicts to declare.

ACKNOWLEDGMENTS

This work was financially supported by Foundation of Jiangsu High Education Committee for Natural Science Research Projects (18KJB150005), the Postdoctoral Science Foundation in Jiangsu province (2018K275C), Changzhou technology programme (CJ20190057), the Natural Science Foundation of Jiangsu Province (BK20190933) and Natural Science Fundamental Research Project of Jiangsu Colleges and Universities (18KJD150005). And there are no conflicts to declare.

REFERENCES

[1] Sivalingam Suganya, Sivan Velmathi, Davoodbasha MubarakAli. Highly selective chemosensor for nano molar detection of Cu^{2+} ion by fluorescent turn-on response and its application in living cells [J]. Dyes and Pigments, 2014, 104:116-122.

[2] Cheng Xingwen, Zhou Yi , Fang Yuan, et al. Multichannel detection of Cu^{2+} based on a rhodamine–ethynylferrocene conjugate [J]. RSC Advances, 2015 5 (25): 19465-19469.

[3] Li Zhanxian, Zhang Lifeng , Li Xiaoya, et al. A fluorescent color/intensity changed chemosensor for Fe^{3+} by photo-induced electron transfer (PET) inhibition of fluoranthene derivative [J]. Dyes and Pigments, 2012 94 (1) :60-65.

[4] Meng Qingtao, Zhang Xiaolin, He Cheng , et al. Multifunctional Mesoporous Silica Material Used for Detection and Adsorption of Cu^{2+} in Aqueous Solution and Biological Applications in vitro and in vivo [J]. Advanced Functional Materials, 2010, 20 (12): 1903-1909.

[5] Masatoshi Ishida, Yoshinori Naruta, Fumito Tani, et al. A Porphyrin-Related Macrocycle with an Embedded 1,10-Phenanthroline Moiety: Fluorescent Magnesium(II) Ion Sensor [J]. Angewandte Chemie International Edition, 2010, 49 (1): 91-94.

[6] Suban K Sahoo, Darshna Sharma, Rati Kanta Bera, et al. Iron(III) selective molecular and supramolecular fluorescent probes [J]. The Royal Society of Chemistry. 2012, 41 (21): 7195-7227.

[7] Philip Aisen, Marianne Wessling-Resnick, Elizabeth A Leibold. Iron metabolism [J]. Current Opinion in Chemical Biology, 1999, 3 (2): 200-206.

[8] Ma Siyue, Yang Zheng, She Mengyao, et al. Design and synthesis of functionalized rhodamine based probes for specific intracellular fluorescence imaging of Fe^{3+} [J]. Dyes and Pigments,2015, 115: 120-126.

ISSN: 2472-3703 DOI: 10.6911/WSRJ.202105_7(5).0027

[9] Li Hongda, Li Liangliang, Yin Bingzhu. Highly selective fluorescent chemosensor for Fe^{3+} detection based on diaza-18-crown-6 ether appended with dual coumarins [J]. Inorganic Chemistry Communications,2014, 42: 1-4.

[10] Yeshwant Ramchandra Bhorge, Haw-Tyng Tsai, Keh-Feng Huang, et al. A new pyrene-based Schiff-base: A selective colorimetric and fluorescent chemosensor for detection of Cu(II) and Fe(III) [J]. Spectrochimica Acta Part A: Molecular and Biomolecular Spectroscopy, 2014, 130: 7-12.

[11] Danuta S. Kalinowski, Des R. Richardson. Future of ToxicologysIron Chelators and Differing Modes of Action and Toxicity: The Changing Face of Iron Chelation Therapy [J]. Chemical Research in Toxicology, 2007,20 (5) : 715-720.

[12] Carlo Brugnara. Iron Deficiency and Erythropoiesis: New Diagnostic Approaches [J]. Clinical Chemistry, 2003, 49 (10): 1573-1578.

[13] Bruno Galy, Dunja Ferring, Belen Minana, et al. Altered body iron distribution and microcytosis in mice deficient in iron regulatory protein 2 (IRP2) [J]. Blood,2005,106 (7): 2580-2589.

[14] Gyeong Jin Park, In Hong Hwang, Eun Joo Song, et al. A colorimetric and fluorescent sensor for sequential detection of copper ion and cyanide [J]. Tetrahedron, 2014, 70 (17): 2822-2828.

[15] Zhang Zhaomin, Shi Yupeng, Pan Yi, et al. Quinoline derivative-functionalized carbon dots as a fluorescent nanosensor for sensing and intracellular imaging of Zn^{2+} [J]. Journal of Materials Chemistry B, 2014, 2(31): 5020-5027.

[16] Janet Y. Uriu-Adams, Carl L. Keen. Copper, oxidative stress, and human health [J]. Molecular Aspects of Medicine, 2005, 26 (4-5): 268-298.

[17] Erik Madsen, Jonathan D. Gitlin. Copper and Iron Disorders of the Brain [J]. Annual Review of Neuroscience, 2007 30 (1): 317-337.

[18] He Xingxing, Zhang Jing, Liu Xungao, et al. A novel BODIPY-based colorimetric and fluorometric dual-mode chemosensor for Hg^{2+} and Cu^{2+} [J]. Sensors and Actuators B: Chemical, 2014, 192: 29-35.

[19] Debajyoti Pramanik, Chandradeep Ghosh, Somdatta Ghosh Dey. Heme-Cu Bound Aβ Peptides: Spectroscopic Characterization, Reactivity, and Relevance to Alzheimer's Disease [J]. Journal of the American Chemical Society, 2011, 133 (39): 15545-15552.

[20] Emily L. Que, Dylan W. Domaille, Christopher J. Chang .Metals in Neurobiology: Probing Their Chemistry and Biology with Molecular Imaging [J]. Chemical Reviews, 2008, 108 (5): 1517-1549.

[21] S. Lunvongsa, M. Oshima, S. Motomizu. Determination of total and dissolved amount of iron in water samples using catalytic spectrophotometric flow injection analysis [J]. Talanta,2006, 68 (3): 969-973.

[22] D.M.C. Gomesa, M.A. Segundoa, J.L.F.C. Lima, et al. Spectrophotometric determination of iron and boron in soil extracts using a multi-syringe flow injection system [J]. Talanta,2005, 66 (3): 703-711.

[23] Andrei R. Timerbaev, Ewa Dabek-Zlotorzynskab, Marc A. G. T. van den Hoop. Inorganic environmental analysis by capillary electrophoresis [J]. Analyst, 1999 124 (6): 811-826.

[24] P. Vanloot, B. Coulomb, C. Brach-Papa, et al. Multivariate optimization of solid-phase extraction applied to iron determination in finished waters [J]. Chemosphere, 2007, 69 (9): 1351-1360.

[25] Tayebeh Shamspur, Iran Sheikhshoaie, Mohamad Hossein Mashhadizadeh. Flame atomic absorption spectroscopy (FAAS) determination of iron(III) after preconcentration on to modified analcime zeolite with 5-((4-nitrophenylazo)-N-(20, 40-dimethoxyphenyl))salicylaldimine by column method [J]. J Anal Atom Spectrom, 2005, 20 (5): 476-478.

ISSN: 2472-3703 DOI: 10.6911/WSRJ.202105_7(5).0027

[26] Geng Jiao, Liu Yuan, Li Jianhui, et al. A ratiometric fluorescent probe for ferric ion based on a 2,2'-bithiazole derivative and its biological applications [J]. Sensors and Actuators B: Chemical, 2006, 222: 612-617.

[27] Pierre-Edouard Danjou, Joël Lyskawa , Francois Delattre , et al. New fluorescent and electropolymerizable N-azacrown carbazole as a selective probe for iron (III) in aqueous media [J]. Sensors and Actuators B: Chemical, 2012, 171-172: 1022-1028.

[28] Li Peng, Zhao Yang, Yao Liang, et al. A simple, selective, fluorescent iron(III) sensing material based on peripheral carbazole [J]. Sensors and Actuators B: Chemical, 2014, 191: 332-336.

[29] Atul Goel, Shahida Umar, Pankaj Nag, et al. A Dual Colorimetric-Ratiometric Fluorescent Probe NAP-3 for Selective Detection and Imaging of Endogenous Labile Iron (III) Pools in C. elegans [J]. Chemical Communications, 2015, 51 (24): 5001-5004.

[30] Yang Liang, Yang Wen, Xu Dongmei, et al. A highly selective and sensitive Fe^{3+} fluorescent sensor by assembling three 1,8-naphthalimide fluorophores with a tris(aminoethylamine) ligand [J]. Dyes and Pigments, 2013, 97 (1): 168-174.

[31] Zhang Shanshan, Sun Tao, Xiao Dejun, et al. A dual-responsive colorimetric and fluorescent chemosensor based on diketopyrrolopyrrole derivative for naked-eye detection of Fe^{3+} and its practical application [J]. Spectrochimica Acta Part A: Molecular and Biomolecular Spectroscopy, 2018, 189: 594-600.

[32] Priya Ranjan Sahoo, Satish Kumar. The experimental and theoretical studies of a merocyanine form based turn off fluorescent sensor for Fe3+ ions with nanomolar level sensitivity in aqueous solution [J]. Journal of Luminescence, 2018, 201: 203-210.

[33] Yang Min, Sun Mingtai , Zhang Zhongping, et al. A novel dansyl-based fluorescent probe for highly selective detection of ferric ions [J]. Talanta, 2013, 105: 34-39.

[34] Jiang Kai, Wu Yancheng, Wu Hanqing, et al. A highly selective, pH-tolerable and fast-response fluorescent probe for Fe^{3+} based on star-shape benzothiazole derivative [J]. Journal of Photochemistry and Photobiology A: Chemistry, 2018, 350: 52-58.

[35] He Yi, Yin Jun, Wang Guang. New selective ''on-off'' fluorescence chemosensor based on carbazole Schiff base for Fe^{3+} detection [J]. Chemistry of Heterocyclic Compounds, 2018, 54 (2): 146-152.

[36] Meng Xianglong, Zhang Xian, Yao Jinshui, et al. Fluorescence and fluorescence imaging of two Schiff derivatives sensitive to Fe^{3+} induced by single- and two-photon excitation [J]. Sensors and Actuators B: Chemical, 2013, 176: 488-496.

[37] Wang Hui, Fang Bin, Zhou Le, et al. A reversible and highly selective two-photon fluorescence "on-off- on" probe for biological Cu^{2+} detection [J]. Organic & Biomolecular Chemistry, 2018, 16(13): 2264-2268.

[38] Wang Guimei, Chen Hangqing, Chen Yaqing, et al. A near-infrared squaraine dye for cascade recognition of copper ion and biological phosphate and its application in IMPLICATION logic gate [J]. Sensors and Actuators B: Chemical, 2016, 233: 550-558.

[39] Yan Zhengquan, Zhu Yanjie, Xu Jie, et al. A novel polydentate Schiff-base derivative developed for multiwavelength colorimetric differentiation of trace Fe^{2+} from Fe^{3+} [J]. Analytical Methods, 2017, 9 (44): 6240-6245.

[40] Yue Wang, Can Wang, Su Xue, et al. High selective and sensitive colorimetric and fluorescent chemosensor of Fe^{3+} and Cu^{2+} based on 2,3,3-trimethylnaphto[1,2-d] squaraine [J]. RSC Advances, 2016, 6(8): 6540-6550 .

ISSN: 2472-3703 DOI: 10.6911/WSRJ.202105_7(5).0027

[41] Hu Lei, Yan Zhengquan, Xu Hongyao. Advances in synthesis and application of near-infrared absorbing squaraine dyes [J]. RSC Advances, 2013, 3 (21): 7667-7676.

[42] Li Benhao, Li Weiwei, Xu Yongqian, et al. A simple approach for the discrimination of surfactants based on the control of squaraine aggregation [J]. Chemical communications, 2015, 51 (78): 14652-14655.